frontiers in Pharmacology

ORIGINAL RESEARCH
published: 28 May 2019
doi: 10.3389/fphar.2019.00571

Characterization of the Metabolic Fate of *Datura metel* Seed Extract and Its Main Constituents in Rats

Cong Xia[1†], Yan Liu[2†], Hai Qi[3], Lulu Niu[1], Yuxuan Zhu[1], Wanying Lu[1], Xinyi Xu[1], Yongjian Su[1], Bingyou Yang[2] and Qi Wang[1*†]*

[1] Department of Medicinal Chemistry and Natural Medicine Chemistry, College of Pharmacy, Harbin Medical University, Harbin, China, [2] Key Laboratory of Chinese Materia Medica, Heilongjiang University of Chinese Medicine, Harbin, China, [3] Department of Cardiology, The 2nd Affiliated Hospital of Harbin Medical University, Harbin, China

Datura metel L. has been frequently used in Chinese traditional medicine. However, little is known on the chemical composition and *in vivo* metabolism of its seeds. In this study, using the strategy "chemical analysis, metabolism of single representative compounds, and metabolism of extract at clinical dosage" that we propose here, 42 constituents were characterized from *D. metel* seeds water extract. Furthermore, the metabolic pathways of 13 representative bioactive compounds of *D. metel* seeds were studied in rats after the oral administration of *D. metel* seeds water extract at a clinical dosage (0.15 g/kg). These included three withanolides, two withanolide glucosides, four amides, one indole, one triterpenoid, one steroid, and one sesquiterpenoid, and with regard to phase II metabolism, hydroxylation, (de)methylation, and dehydrogenation reactions were dominant. Furthermore, the metabolism of *D. metel* seeds water extract provided to rats at a clinical dosage was investigated by liquid chromatography-tandem mass spectrometry based on the above metabolic pathways. Sixty-one compounds were detected in plasma, 83 in urine, and 76 in fecal samples. Among them, withanolides exhibited higher plasma exposure than the other types. To our knowledge, this is the first systematic study on the chemical profiling and metabolite identification of *D. metel* seeds, including all compounds instead of single constituents.

Keywords: *Datura metel* seeds, metabolites identification, LC–MS fingerprinting, withanolides, amides, indoles

OPEN ACCESS

Edited by:
Haitao Lu,
Shanghai Jiao Tong University, China

Reviewed by:
Eva Maria Pferschy-Wenzig,
University of Graz, Austria
Johanna Mahwahwatse Bapela,
University of Pretoria, South Africa

***Correspondence:**
Bingyou Yang
ybywater@163.com
Qi Wang
mydearmumu@163.com

† These authors have contributed equally to this work

Specialty section:
This article was submitted to Ethnopharmacology, a section of the journal Frontiers in Pharmacology

Received: *30 November 2018*
Accepted: *06 May 2019*
Published: *28 May 2019*

Citation:
Xia C, Liu Y, Qi H, Niu L, Zhu Y, Lu W, Xu X, Su Y, Yang B and Wang Q (2019) Characterization of the Metabolic Fate of Datura metel Seed Extract and Its Main Constituents in Rats. Front. Pharmacol. 10:571. doi: 10.3389/fphar.2019.00571

INTRODUCTION

Datura metel L. (Solanaceae) seeds are one of the most popular herbal medicines for the treatment of rheumatoid arthritis and convulsions (Murthy et al., 2004). Although the seeds are toxic, they also have strong analgesic, anthelmintic, antioxidant, antimicrobial, antiviral, and antidiabetic activities (Wannang and Ndukwe, 2009; Kamaraj et al., 2011; Gu et al., 2014; Bachheti et al., 2018; Roy et al., 2018). Withanolides, flavonoids, alkaloids, sesquiterpenoids, lignans, and phenolic acids are generally considered the major bioactive compounds of *D. metel* (Kuang et al., 2008; Mai et al., 2017). However, there are few reports on the chemical composition of *D. metel* seeds. In previous studies, amides, indoles, sesquiterpenes, withanolides, and withanolide glucosides have been isolated from *D. metel* (Yang et al., 2010a,b; Bellila et al., 2011), but the constituents responsible for the treatment of different conditions have not been clarified.

It is well known that the *in vivo* metabolites of herbal medicines may play a substantial role in the therapeutics. Therefore, metabolites' identification is critical for elucidating the bioactivities of complex herbal medicines. Recently, we studied the metabolism of two typological components, including two amides (*n*-trans-feruloyltyramine and cannabisin F) and two withanolide glucosides (daturataturin A and daturametelin I) of *D. metel* seeds in rats (Xu et al., 2018). To fully predict and identify their metabolites, we selected seven main types of representative compounds from the seeds.

In this study, we aimed to improve this strategy so that it can be applied to other herbal medicines. Focusing on the identification of the *in vivo* metabolites of *D. metel* seed extracts after oral administration in rats, we first established the chemical fingerprint of *D. metel* seeds and identified 42 seed components (**Figure 1**). Second, we examined the *in vivo* metabolic pathways of seven groups of metabolites with different scaffolds, which included 13 representative compounds, using quadrupole time-of-flight mass spectrometry (qTOF-MS) and liquid chromatography-tandem mass spectrometry (LC/MS/MS). Finally, a normal clinical dosage of the herbal extract was administered to rats, and several metabolites were detected based on the metabolic pathways. Following this strategy, 113 metabolites (including 42 original phytochemicals and 71 newly formed ones) were detected at a clinical dosage (0.15 g/kg) in rats.

MATERIALS AND METHODS

Chemicals and Reagents

The pure compounds daturametelindole B (**1**), daturametelin M (**3**), hyoscyamilactol (**5**), daturametelindole A (**9**), daturametelin L (**29**), daturametelindole D (**18**), *n*-trans-feruloyltyramine (**19**), daturametelindole C (**22**), daturametelin I (**30**), cannabisin F (**31**), daturaolone (**32**), daturataturin A (**36**), *n*-trans-p-coumaroyltyramine (**40**), and stigmasterol (**41**) were isolated from the seeds of *D. metel* by the authors. Their structures were characterized using nuclear magnetic resonance and MS (**Figure 2** and **Supplementary Figures S3–S22**; Xu et al., 2018). Dinoxin B (**10**), withametelin L (**13**), and cinerolide (**20**) were purchased from Nantong Feiyu Biological Technology Co., Ltd. (Nanjing, China). Purities were above 98% according to high-performance liquid chromatography-ultraviolet (HPLC/UV) analysis. Beta-glucuronidase (HP-2 type, containing 100,000 U β-glucuronidase and 7500 U sulfatase per milliliter), β-nicotinamide adenine dinucleotide phosphate hydrate (β-NADP), D-glucose 6-phosphate sodium salt (G-6-P), and glucose-6-phosphate dehydrogenase (G-6-P-DE) used in the present study were purchased from Sigma–Aldrich (St. Louis, MO, United States). Heparin was purchased from HuiShi Biochemical Reagent Co., Ltd. (Shanghai, China). De-ionized water was prepared by a Milli-Q system (Millipore, Burlington, MA, United States). Acetonitrile, methanol, and formic acid (Sigma–Aldrich) were of HPLC grade. Other reagents were of analytical grade.

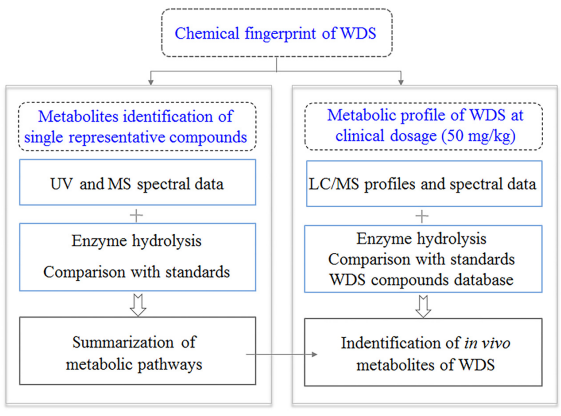

FIGURE 1 | The three-step strategy proposed in the present study.

Preparation of the Water Decoction of *Datura metel* Seeds (WDS)

Datura metel seeds were collected from the medicinal botanical garden of Heilongjiang University of Traditional Chinese Medicine. The authenticity of the sample was identified by Dr. Ruifeng Fan, Botanist, Department of Medicinal Plant, Heilongjiang University of Traditional Chinese Medicine. The voucher specimen (specimen number: 2016035) were preserved in the laboratory of Chinese Medicine Chemistry, Heilongjiang University of Traditional Chinese Medicine. The WDS was prepared by extracting 100 g of *D. metel* seeds decocted in 600 mL water three times (2.0, 2.0, 1.0 h). The decoctions were combined, filtered, and concentrated in vacuum at 50°C. The final concentration of the extract was 0.01 g/mL (crude drug per g/mL).

Animals and Drug Administration

Male Sprague–Dawley rats (180–220 g) were purchased from the Laboratory Animal Center of the Second Affiliated Hospital of Harbin Medical University (Heilongjiang Province, China). The rats were kept in metabolic cages (465 mm × 300 mm × 200 mm), and the breeding room was at 25°C and 60 ± 5% relative humidity. All animals had free access to water and normal chow was provided *ad libitum* at a 12 h dark–light cycle for 3 days, and then fasted for 12 h before the experiments. The animal facilities and protocols were approved by the Animal Care and Use Committee of the Harbin Medical University. All procedures were in accordance with the National Institutes of Health Guide for the Care and Use of Laboratory Animals (ILAR, 1996).

The pure compounds, including **1**, **3**, **5**, **9**, **10**, **13**, **18**, **20**, **22**, **29**, **32**, **40**, and **41**, were suspended in 1% carboxy-methyl cellulose-sodium and were separately provided to rats (n = 4) orally at 20 mg/kg. The WDS was provided to rats (n = 4) at 0.5 g/kg (clinical dosage, equivalent to 600 mg/day for a 60-kg human), respectively. The dosage in our study was the clinically safe and effective (Pharmacopoeia Commission, 2015). The control group (n = 4) was administrated with 1000 μL normal saline.

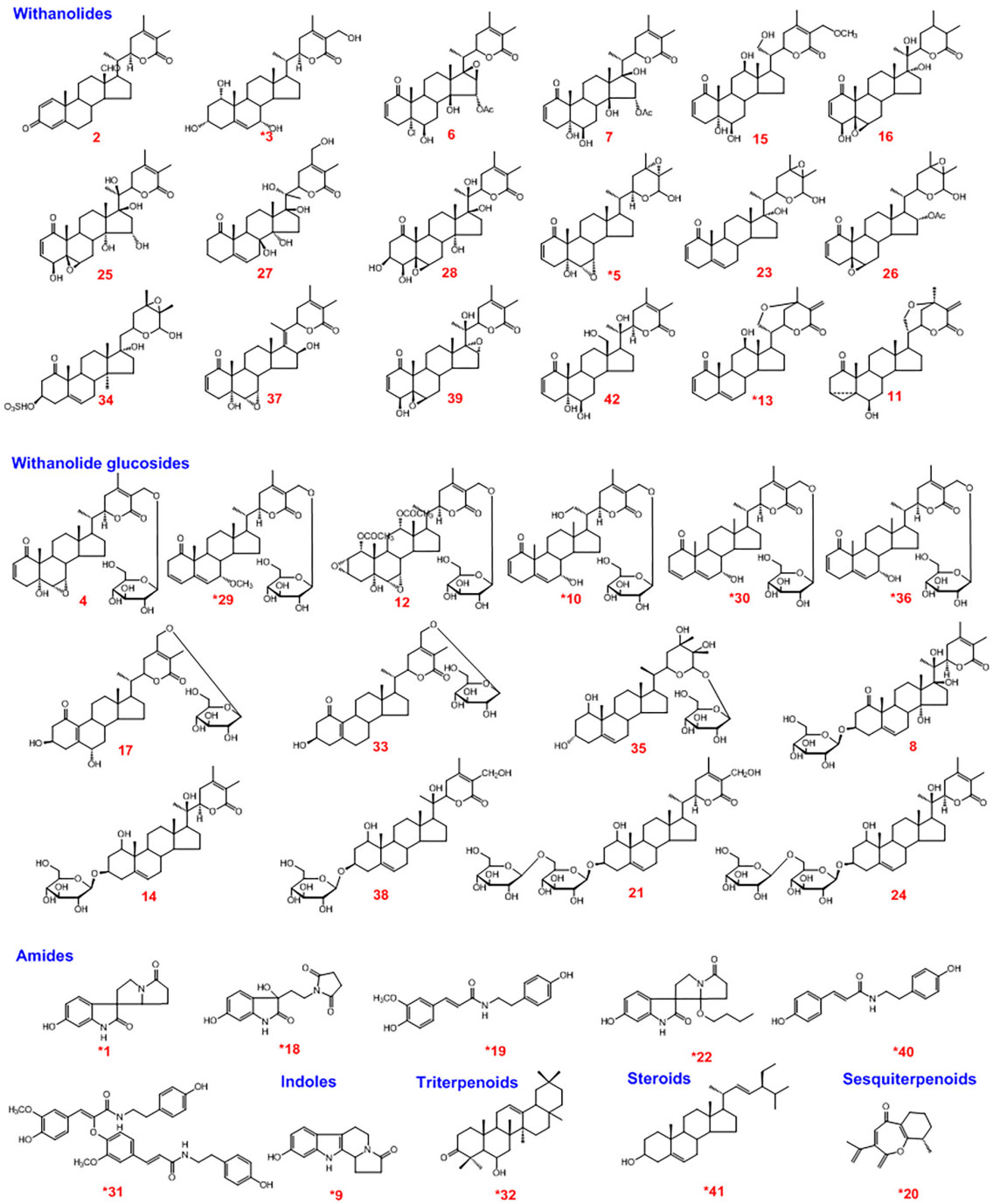

FIGURE 2 | Structure of the chemical constituents of the water extract of *Datura metel* seeds (WDS).*Identified by comparing with reference standards.

Preparation of Plasma, Urine, and Fecal Samples

To obtain plasma samples, blood (1000 μL) was collected from the angular vein into heparinized tubes at six time points: 0.5, 1, 2, 4, 6, and 10 h after the administration of WDS and pure compounds (n = 4). The blood of two rats was collected at 0.5, 2, and 6 h, or at 1, 4, and 10 h, and then centrifuged at 10,000 × g for 10 min at 4°C to obtain the plasma and then pooled plasma samples of different time points. Urine and fecal samples were collected for 0–24 h from rats held in metabolic cages (DXL-D, Keke Medical Model Co., Ltd., Shanghai, China).

Plasma, urine, and fecal samples were prepared as described in our previous report (Xu et al., 2018). The residue of these samples was dissolved in 300 μL of methanol, and filtered

through a 0.22-μm membrane for ultra-high performance liquid chromatography coupled with electrospray ionization (UPLC/ESI) qTOF-MS analysis.

Incubation of Rat Liver Microsomes

Compounds **3**, **5**, **10**, **13**, **29**, **40**, and **41** were separately dissolved in methanol, and then diluted with phosphate buffered saline (PBS). The final concentration of each compound in the 200-μL incubation mixture (NADPH-generating system, 100 mM potassium phosphate buffer (pH 7.4), and rat liver microsomes) was 25 μM, and the amount of organic solvent in the mixture was lower than 1% (v/v). PBS-containing methanol was added as the negative control. The incubation was conducted at 37°C for 2 h. After this period, the reaction was terminated by adding 1000 μL of cold acetonitrile. The mixture was then kept at 4°C for 30 min, and the precipitated protein was removed by centrifugation at 10,000 × *g* for 10 min at 4°C.

Enzyme Hydrolysis

A 100-μL aliquot of plasma or urine sample was dried under a gentle flow of nitrogen gas and then mixed with 400 μL of b-glucuronidase solution (containing 19.86 U/μL, in sodium acetate buffer, pH 5.5). The mixture was vortexed for 5 min, incubated in a 37°C water bath for 1.5 h, treated with 1000 μL of cold methanol–acetonitrile (1:1, v/v) to precipitate the protein, and then centrifuged at 10,000 × *g* for 10 min at 4°C. The supernatant was dried under a gentle nitrogen flow and then dissolved in 100 μL of methanol. The solution was filtered through a 0.22-μm membrane for analysis.

UPLC/ESI/qTOF-MS Analysis

The analysis was performed on an ACQUITY UPLC instrument coupled with a Xevo G2 qTOF mass spectrometer (Waters, Milford, MA, United States) via an ESI ion source. The autosampler was controlled via the MassLynx^{TM} 4.1 software (Waters). Samples were separated on an ACQUITY UPLC HSS T3 column (2.1 mm × 100 mm, 1.7 μm; Waters). The mobile phase consisted of acetonitrile (A) and water containing 0.1% (v/v) formic acid (B) at a flow rate of 400 μL/min. The gradient elution program was set as follows: 0–7 min, 10–22% A; 7–13 min, 22–70% A; 13–17 min, 70–90% A; 17–20 min, 90–95% A; 20–22 min, 95% A. A 2-μL sample aliquot was injected for analysis, and the column temperature was 40°C.

The qTOF/MS system was equipped with an ESI source operating in positive ion mode, as in our previous report (Xu et al., 2018). High-purity nitrogen (N_2) and high-purity helium (He) were used as desolvation gas and collision gas, respectively. The flow rate of N_2 was 600 L/h and that of He was 50 L/h. The optimized parameters were: capillary voltage, 3.5 kV; sample cone voltage, 30 V; and extraction cone voltage, 4 V. The desolvation and source temperatures were 350°C and 100°C, respectively. The MS full scan range was 100–1000 *m*/*z*, and MS^n range was 100–800 *m*/*z*. All data collected in the positive ion mode were acquired and processed by the MassLynx^{TM} 4.1 software (Waters). UHPLC/qTOF-MS is the high-resolution mass spectra, which could provide the accurate $[M+H]^+$ ions of the metabolites.

Quadrupole Ion Trap (Q TRAP) LC/MS/MS

The AB SCIEX 4000 Q TRAP^{TM} composite triple quadrupole/linear ion trap tandem mass spectrometer (SCIEX, Framingham, MA, United States) connected to the UHPLC via the ESI interface (Applied Biosystems, Foster City, CA, United States) was operated in the positive ion mode. The column effluent was split using a zerodead-volume "T" connector, with approximately half of the flow being fed to the mass spectrometer. The interface and parameters of the mass spectrometer were as follows: spray capillary voltage, 5.5 kV; DP, 70 V; EP, 0 V; CE, 45 V; nebulizer pressure, 40 psi; dry gas pressure, 40 psi; curtain gas pressure, 10 psi; and dry gas temperature, 600°C. All data were acquired and processed using Analyst (SCIEX). The mass spectrum fragment ions of MS^2 and MS^3 could be obtained by Q-TRAP LC/MS/MS.

RESULTS AND DISCUSSION

Characterization of the Chemical Constituents of WDS

A rapid and sensitive UHPLC/qTOF-MS method was employed to characterize the chemical constituents of WDS. Forty-two compounds (**1**–**42**) were identified or tentatively characterized

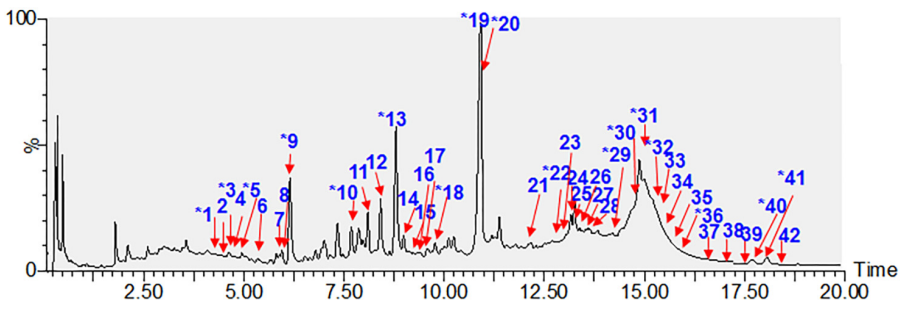

FIGURE 3 | LC/MS total ion currents of the water extract of *Datura metel* seeds (WDS). *Identified by comparing with reference standards.

TABLE 1 | Characterization of *in vivo* metabolites of *Datura metel* seeds by UPLC/ESI/qTOF-MS and Q-Trap LC/MS/MS in this study.

No.	RT	Formula	HR-MS [M+H]$^+$			(+)ESI-MS^n(*m/z*)	Metabolic Reaction	Plasma	Urine	Feces	
	(min)		Measured	Predicted	Δ (ppm)						Source
***1**	4.32	$C_{14}H_{14}N_2O_3$	259.1072	259.1077	1.9	MS^2[259]: 240,162,150,114	Daturametelindole B	−	−	+	D^S,D^W
[a] 1-M1	3.17	$C_{20}H_{22}N_2O_9$	453.1405	453.1398	−1.5	MS^2[453]: 340,150 MS^3[150]: 114	+GluA	+	++	++	D^S,D^W
1-M2	3.68	$C_{14}H_{14}N_2O_6S$	339.0652	339.0645	−2.1	MS^2[339]: 321,150 MS^3[150]: 122,114	+Sul	++	+	−	D^S,D^W
1-M3	5.28	$C_{14}H_{12}N_2O_3$	257.0913	257.0921	3.1	MS^2[257]: 150,136,122	−2H	−	+	−	D^S
2	4.48	$C_{28}H_{36}O_4$	437.2689	437.2686	−0.7	MS^2[437]: 283,258,240,150	Paraminabeolide A	+	+	−	D^W
***3**	4.52	$C_{28}H_{42}O_6$	475.3022	475.3054	6.7	MS^2[475]: 305,135,170	Daturametelins M	+	+	−	D^S,D^W
3-M1	4.03	$C_{28}H_{40}O_5$	457.2956	457.2949	−1.5	MS^2[457]: 287,163,149	-H_2O	+	+	++	D^S,D^W
3-M2	4.24	$C_{28}H_{44}O_8$	509.3112	509.3109	−0.6	MS^2[509]: 340,136	+H_2O+OH	+	+	++	D^S,D^W
3-M3	4.36	$C_{28}H_{42}O_7$	491.3001	491.3003	−0.4	MS^2[491]: 323,155,135	+OH	+	+	−	D^S,D^W
3-M4	4.42	$C_{29}H_{44}O_6$	489.3229	489.3212	−3.4	MS^2[489]: 319,136	+CH_3	−	+	+	D^S
4	4.54	$C_{34}H_{48}O_{11}$	633.3274	633.3269	−0.8	MS^2[633]: 469,453,203,150	Baimantuoluoside C	+	−	−	D^W
4-M1	3.69	$C_{33}H_{46}O_{14}S$	699.2673	699.2681	1.1	MS^2[699]: 619,455 MS^3[455]: 273,187,163,136	+Sul-CH_3	+	+	−	D^W
4-M2	4.18	$C_{34}H_{46}O_{11}$	631.3119	631.3113	−1.0	MS^2[631]: 467,288,136	−2H	−	++	−	D^W
4-M3	4.35	$C_{40}H_{56}O_{17}$	809.3598	809.3590	−0.9	MS^2[809]: 633,469,295,136	+GluA	−	++	−	D^W
***5**	4.60	$C_{28}H_{40}O_6$	473.2887	473.2898	2.3	MS^2[473]: 301,206,171	Hyoscyamilactol	+	+	++	D^S,D^W
5-M1	4.13	$C_{28}H_{40}O_7$	489.2838	489.2847	1.8	MS^2[489]: 338,317,171,135	+OH	++	+	+	D^S,D^W
6	5.38	$C_{30}H_{39}ClO_8$	563.2412	563.2406	−1.0	MS^2[563]: 409,393,260,153	Physagulin I	+	+	+	D^W
6-M1	4.31	$C_{30}H_{39}ClO_{11}S$	643.1985	643.1974	−1.7	MS^2[643]: 563,409,164	+Sul	−	+	+	D^W
6-M2	4.95	$C_{36}H_{45}ClO_{14}$	737.2583	737.2571	−1.6	MS^2[737]: 561,407,150	+GluA-2H	−	−	+	D^W
7	5.86	$C_{30}H_{42}O_9$	547.2879	547.2902	4.2	MS^2[547]: 393,240,153,114	Physagulin K	−	+	+	D^W
8	5.92	$C_{34}H_{50}O_{12}$	651.3371	651.3375	0.6	MS^2[651]: 487,319,288,163	Coagulin L	+	+	−	D^W
***9**	6.12	$C_{14}H_{14}N_2O_2$	243.1116	243.1128	4.9	MS^2[243]: 215,187,107	Daturametelindole A	+	+	+	D^S,D^W
[a] 9-M1	2.75	$C_{20}H_{20}N_2O_8$	417.1297	417.1292	−1.2	MS^2[417]: 241,150,134	+GluA-2H	−	−	++	D^S,D^W
[a] 9-M2	4.69	$C_{20}H_{22}N_2O_9$	435.1388	435.1398	2.3	MS^2[435]: 259,231,136	+GluA+OH	++	+	−	D^S,D^W
9-M3	5.28	$C_{15}H_{16}N_2O_2$	257.1296	257.1285	−4.2	MS^2[257]: 243,215,136,107	+CH_3	+	+	++	D^S,D^W
[a] 9-M4	5.82	$C_{20}H_{22}N_2O_{11}S$	499.1002	499.1017	3.0	MS^2[499]: 419,243,150	+GluA+Sul	+	+	−	D^S,D^W
9-M5	6.49	$C_{13}H_{12}N_2O_5S$	309.0532	309.0540	2.5	MS^2[309]: 229,136,122	+Sul-CH_3	++	+	−	D^S,D^W
9-M6	6.68	$C_{14}H_{14}N_2O_6S$	339.0652	339.0645	−2.0	MS^2[339]: 259,243,215	+Sul+OH	++	++	−	D^S,D^W
***10**	7.52	$C_{34}H_{48}O_{11}$	633.3244	633.3269	3.9	MS^2[633]: 469,437 MS^3[469]: 285,136	Dinoxin B	+	++	+	D^S,D^W
10-M1	5.88	$C_{34}H_{48}O_{12}$	649.3251	649.3219	−4.9	MS^2[649]: 483,299,136	+OH	+	++	+	D^S,D^W
10-M2	6.03	$C_{35}H_{50}O_{11}$	647.3442	647.3426	−2.4	MS^2[647]: 483,471,285	+CH_3	+	+	++	D^S,D^W
[a] 10-M3	7.06	$C_{40}H_{56}O_{17}$	809.3586	809.3590	0.5	MS^2[809]: 437,469,246,136	+GluA	+	++	++	D^S,D^W

(Continued)

TABLE 1 | Continued

No.	RT	Formula	HR-MS $[M+H]^+$			(+)ESI-MS^n(*m/z*)	Metabolic Reaction	Plasma	Urine	Feces	
	(min)		Measured	Predicted	Δ (ppm)						Source
10-M4	8.44	$C_{34}H_{46}O_{11}$	631.3132	631.3113	−3.0	MS^2[632]: 467,421,228,114	-2H	+	+	+	D^S,D^W
10-M5	9.78	$C_{28}H_{35}O_6$	468.2533	468.2506	−5.7	MS^2[468]: 283,134	-Glc-2H	−	+	+	D^S,D^W
11	8.14	$C_{28}H_{38}O_5$	455.2799	455.2792	−1.5	MS^2[455]: 287,167,152,135	Withawrightolide	−	−	+	D^W
12	8.36	$C_{38}H_{54}O_{15}$	751.3517	751.3535	2.3	MS^2[751]: 589,419,331,193	Chantriolide C	−	−	+	D^W
12-M1	8.51	$C_{44}H_{62}O_{21}$	927.3855	927.3856	0.1	MS^2[927]: 751,589,419 MS^3[419]: 331,193,155,134	+GluA	−	−	++	D^W
12-M2	7.58	$C_{37}H_{52}O_{18}S$	817.2951	817.2947	−0.5	MS^2[817]: 737,575,405,193	+Sul-CH_3	−	−	+	D^W
12-M3	7.62	$C_{38}H_{56}O_{17}$	785.3573	785.3590	2.1	MS^2[785]: 391,357,193,163	+OH+H_2O	−	−	++	D^W
12-M4	8.00	$C_{39}H_{56}O_{16}$	781.3628	781.3641	1.6	MS^2[781]: 391,373,355,193,163	+OH+CH_3	−	−	++	D^W
12-M5	14.98	$C_{38}H_{52}O_{15}$	749.3361	749.3379	2.4	MS^2[749]: 357,283,193,163	-2H	−	−	++	D^W
***13**	8.73	$C_{28}H_{36}O_5$	453.2654	453.2636	−3.9	MS^2[453]: 341,285,167,114	Withametelin L	++	++	++	D^S,D^W
13-M1	7.74	$C_{27}H_{34}O_8S$	519.2055	519.2047	−1.5	MS^2[519]: 439,271,167,150	+Sul-CH_3	+	+	+	D^S,D^W
13-M2	8.19	$C_{28}H_{36}O_6$	469.2574	469.2585	2.3	MS^2[469]: 301,269,167	+OH	++	++	++	D^S,D^W
14	8.91	$C_{34}H_{52}O_{10}$	621.3642	621.3633	−1.4	MS^2[621]: 509,457 MS^3[457]: 314,287,163,135	Coagulin Q	+	+	+	D^W
15	9.05	$C_{29}H_{42}O_8$	519.2957	519.2950	−1.3	MS^2[519]: 319,295,262,199,165	Baimantuoluoline C	+	+	+	D^W
15-M1	7.56	$C_{29}H_{42}O_9$	535.2914	535.2902	−2.2	MS^2[535]: 509,335,199,165	+OH	++	+	+	D^W
16	9.40	$C_{28}H_{40}O_7$	489.2856	489.2847	−1.8	MS^2[489]:439,317,353,171	Philadelphicalactone A	−	+	+	D^W
17	9.43	$C_{33}H_{48}O_{11}$	621.3288	621.3269	−3.0	MS^2[621]: 457,289,136	Withalongolide L	+	++	−	D^W
17-M1	7.37	$C_{33}H_{48}O_{14}S$	701.2834	701.2838	−0.5	MS^2[701]: 621,457,289,136	+Sul	−	++	++	D^W
***18**	9.77	$C_{14}H_{14}N_2O_5$	291.0968	291.0975	2.4	MS^2[291]: 246,219,155,135	Daturametelindole D	+	+	++	D^S,D^W
18-M1	7.48	$C_{13}H_{12}N_2O_8S$	357.0391	357.0387	−1.1	MS^2[357]: 277,144,135	+Sul-CH_3	+	+	++	D^S
18-M2	8.43	$C_{14}H_{14}N_2O_8S$	371.0538	371.0544	1.6	MS^2[371]: 291,155,135	+Sul	−	+	++	D^S,D^W
***19**	10.86	$C_{18}H_{19}NO_4$	314.1366	314.1387	6.6	MS^2[314]: 314,177,163	N-trans-feruloyltyramine	−	−	++	D^W
[a] 19-M1	8.50	$C_{24}H_{27}NO_{11}$	506.1669	506.1657	−2.3	MS^2[506]: 330,314,177,145	+GluA+OH	++	+	−	D^W
19-M2	8.14	$C_{18}H_{19}NO_5$	330.1339	330.1336	−0.9	MS^2[330]: 177,137	+OH	++	+	−	D^W
19-M3	9.65	$C_{18}H_{17}NO_4$	312.1232	312.1230	−0.6	MS^2[312]: 177,145,114	-2H	++	++	++	D^W
***20**	10.91	$C_{15}H_{18}O_2$	231.1377	231.1380	1.3	MS^2[231]: 215,203,190,136	Cinerolide	+	+	++	D^S,D^W
[a] 20-M1	6.46	$C_{21}H_{24}O_8$	405.1552	405.1544	−1.9	MS^2[405]: 229,187,201,134	+GluA-2H	+	+	−	D^S,D^W
20-M2	8.60	$C_{15}H_{18}O_5S$	311.0934	311.0948	4.5	MS^2[311]: 231,190,136	+Sul	++	+	−	D^S,D^W
20-M3	9.92	$C_{14}H_{16}O_2$	217.1211	217.1223	5.5	MS^2[217]: 189,174	-CH_3	+	+	−	D^S
21	12.10	$C_{40}H_{62}O_{15}$	783.4153	783.4161	1.0	MS^2[783]: 457,355,325,288	Withanoside IV	−	+	−	D^W
21-M1	8.06	$C_{41}H_{64}O_{16}$	813.4274	813.4267	−0.8	MS^2[814]: 487,325,318,226,288	+OH+CH_3	−	++	++	D^W
***22**	12.87	$C_{18}H_{22}N_2O_4$	331.1660	331.1652	−2.4	MS^2[331]: 325,223,189,107	Daturametelindole C	++	+	−	D^S,D^W
22-M1	8.21	$C_{17}H_{20}N_2O_7S$	397.1068	397.1064	−1.0	MS^2[397]: 317,209,107	+Sul-CH_3	++	++	++	D^S,D^W
22-M2	10.07	$C_{17}H_{20}N_2O_4$	317.1487	317.1496	2.8	MS^2[317]: 209,150,107	-CH_3	++	+	−	D^S,D^W

(Continued)

TABLE 1 | Continued

No.	RT	Formula	HR-MS $[M+H]^+$			(+)ESI-MS^n(*m/z*)	Metabolic Reaction	Plasma	Urine	Feces	
	(min)		Measured	Predicted	Δ (ppm)						Source
23	12.93	$C_{28}H_{40}O_5$	457.2945	457.2949	0.8	MS^2[457]: 285,171,151,147	Cilistol A	−	−	+	D^W
23-M1	8.96	$C_{34}H_{48}O_{11}$	633.3257	633.3269	1.9	MS^2[633]: 457,171,151	+GluA	−	−	+	D^W
24	13.09	$C_{40}H_{62}O_{15}$	783.4154	783.4161	0.9	MS^2[783]: 457,325,289,162	Withanoside VI	−	−	+	D^W
25	13.21	$C_{28}H_{38}O_9$	519.2577	519.2589	2.3	MS^2[520]: 349,197,137	Withangulatin B	−	−	+	D^W
26	13.41	$C_{30}H_{42}O_7$	515.3018	515.3003	−2.9	MS^2[515]: 343,329,193,171,150	Virginol C	−	+	+	D^W
26-M1	15.29	$C_{36}H_{50}O_{14}$	707.3282	707.3273	−1.2	MS^2[708]: 532,359,193,171,166	+GluA+OH	−	++	++	D^W
27	13.48	$C_{28}H_{40}O_8$	505.2786	505.2796	1.9	MS^2[505]: 319,264,185,136	Ajugin D	+	−	−	D^W
27-M1	10.24	$C_{34}H_{48}O_{17}S$	761.2674	761.2685	1.4	MS^2[761]: 585,505,319,185	+GluA+Sul	−	−	++	D^W
28	13.98	$C_{28}H_{40}O_9$	521.2747	521.2745	−0.4	MS^2[521]: 351,255,184,169	Phyperunolide E	−	−	+	D^W
28-M1	4.63	$C_{34}H_{48}O_{15}$	697.3059	697.3066	1.0	MS^2[697]: 521, 351,203,169	+GluA	−	+	−	D^W
28-M2	14.5	$C_{27}H_{38}O_9$	507.2578	507.2589	2.1	MS^2[508]: 351,184,167,155	$-CH_3$	−	+	−	D^W
***29**	14.11	$C_{35}H_{50}O_{10}$	631.3441	631.3477	5.7	MS^2[631]: 566,467 MS^3[467]: 299,162,136	Daturametelin L	−	+	+	D^S,D^W
29-M1	9.60	$C_{35}H_{50}O_{11}$	647.3439	647.3426	−2.0	MS^2[647]: 483,469,285,135	+OH	+	+	−	D^S,D^W
[a] 29-M2	10.61	$C_{41}H_{58}O_{16}$	807.3781	807.3798	2.1	MS^2[807]: 631,453,285,135	+GluA	−	++	++	D^S,D^W
*29-M3	14.93	$C_{34}H_{48}O_{10}$	617.3315	617.3320	0.8	MS^2[617]: 453,441,285,135	$-CH_3$ (**30**)	−	++	+	D^W
29-M4	15.15	$C_{29}H_{37}O_5$	466.2720	466.2714	−1.2	MS^2[466]: 453,285,134	-Glc-2H	−	++	++	D^W
***30**	14.93	$C_{34}H_{48}O_{10}$	617.3312	617.3320	1.3	MS^2[617]: 453, 285,271,135	Daturametelin I	−	++	+	D^W
[a] 30-M1	4.53	$C_{34}H_{48}O_{11}$	633.3242	633.3269	4.2	MS^2[633]: 469,285,136	+OH	−	+	+	D^W
***31**	15.08	$C_{36}H_{36}N_2O_8$	625.2521	625.2544	3.6	MS^2[625]:488,377,298,164,136	Cannabisin F	−	+	++	D^W
[a] 31-M1	8.83	$C_{42}H_{44}N_2O_{15}$	817.2854	817.2814	−4.8	MS^2[817]:641,611,488,373,298	+GluA+OH	−	+	++	D^W
31-M2	9.28	$C_{35}H_{34}N_2O_8$	611.2368	611.2388	3.2	611,474,373,298,136	$-CH_3$	+	+	++	D^W
***32**	15.21	$C_{30}H_{48}O_2$	441.3712	441.3727	3.3	MS^2[441]: 423,357,150	Daturaolone	−	−	++	D^S,D^W
[a] 32-M1	7.54	$C_{36}H_{56}O_9$	633.3999	633.3997	−0.3	MS^2[633]: 457,435,114	+GluA+OH	+	−	−	D^S
33	15.35	$C_{33}H_{48}O_{10}$	605.3317	605.3320	0.4	MS^2[605]: 441,273,148,138	Withalongolide M	−	−	+	D^W
33-M1	7.10	$C_{33}H_{48}O_{14}S$	701.2854	701.2838	−2.2	MS^2[701]: 621,457,289,135	+Sul+OH	++	+	−	D^W
34	15.39	$C_{28}H_{42}O_9S$	555.2606	555.2622	2.8	MS^2[555]: 357,299,150	Cilistol Y	+	+	+	D^W
35	15.53	$C_{34}H_{56}O_{11}$	641.3874	641.3895	3.2	MS^2[642]: 429,385,341,150	Cilistol J	−	−	+	D^W
***36**	15.62	$C_{34}H_{48}O_{10}$	617.3315	617.3320	0.8	MS^2[617]: 453,285,136	Daturataturin A	−	+	+	D^W
*36-M1	7.53	$C_{34}H_{48}O_{11}$	633.3247	633.3269	3.4	MS^2[633]: 469,285,136	+OH (**10**)	++	+	+	D^W
[a] 36-M2	7.82	$C_{40}H_{54}O_{16}$	791.3451	791.3485	4.2	MS^2[791]: 617,451,268,133	+GluA-2H	+	−	−	D^W
36-M3	9.52	$C_{35}H_{50}O_{10}$	631.3496	631.3477	−3.0	MS^2[631]: 453,299,136	$+CH_3$	+	+	−	D^W
36-M4	11.63	$C_{28}H_{36}O_5$	453.2653	453.2636	−3.7	MS^2[454]: 437,283,136	-Glc-2H	+	++	++	D^W
37	16.68	$C_{28}H_{36}O_6$	469.2565	469.2585	4.2	MS^2[469]: 316,270,153,136,122	Exodeconolide A	+	+	+	D^W
38	17.03	$C_{34}H_{52}O_{11}$	637.3568	637.3582	2.1	MS^2[637]: 457,285,185,153	Withanoside XI	−	++	++	D^W
38-M1	8.03	$C_{40}H_{60}O_{17}$	813.3912	813.3903	−1.1	MS^2[813]: 637,457,285,185	+GluA	++	++	++	D^W

(Continued)

TABLE 1 | Continued

No.	RT	Formula	HR-MS $[M+H]^+$			(+)ESI-MS^n(*m/z*)	Metabolic Reaction	Plasma	Urine	Feces	Source
	(min)		Measured	Predicted	Δ (ppm)						
39	17.58	$C_{28}H_{36}O_7$	485.2521	485.2534	2.6	MS^2[485]: 315,176,169,151	20-Hydroxytubocapsanolide A	–	–	+	D^W
***40**	17.74	$C_{17}H_{17}NO_3$	284.1286	284.1281	−1.7	MS^2[284]: 147,136,122	*n*-trans-p-coumaroyltyramine	++	++	++	D^S,D^W
40-M1	10.96	$C_{17}H_{19}NO_5$	318.1358	318.1336	−6.9	MS^2[318]: 274,230,150,114	+OH+H_2O	++	++	++	D^S,D^W
40-M2	12.93	$C_{17}H_{17}NO_4$	300.1211	300.1230	6.3	MS^2[300]: 152,114	+OH	++	+	+	D^S,D^W
[a] 40-M3	13.24	$C_{23}H_{25}NO_9$	460.1623	460.1602	−4.5	MS^2[460]:284,136	+GluA	+	++	++	D^S,D^W
40-M4	14.09	$C_{17}H_{17}NO_6S$	364.0833	364.0849	4.3	MS^2[364]:284,147,136	+Sul	+	++	++	D^S,D^W
40-M5	16.33	$C_{23}H_{23}NO_9$	458.1437	458.1446	1.9	MS^2[458]: 282,147,134	+GluA-2H	–	+	++	D^S,D^W
***41**	18.08	$C_{29}H_{48}O$	413.3790	413.3778	−2.9	MS^2[413]: 273,139,135	Stigmasterol	++	++	–	D^S,D^W
41-M1	8.74	$C_{29}H_{48}O_2$	429.3741	429.3727	−3.2	MS^2[429]: 289,274,139	+OH	++	+	–	D^S,D^W
41-M2	12.08	$C_{29}H_{46}O_3$	443.3509	443.3520	2.4	MS^2[443]: 289,196,153,141,135	+2OH	+	+	–	D^S,D^W
41-M3	13.42	$C_{29}H_{50}O_3S$	479.3563	479.3553	−2.0	MS^2[479]: 399,275,137	+2H+Sul	–	+	++	D^S,D^W
42	18.43	$C_{28}H_{40}O_7$	489.2821	489.2847	5.3	MS^2[489]: 319,169,151	Jaborosalactone VIII	+	–	–	D^W

*, *Identified by comparing with reference standards; ++, detected at high abundance, > 1 × e^4; +, only detected, 1 × e^3 ~ 1 × e^4; –, not detected.* [a] *Confirmed by enzyme hydrolysis. D^S, detected in single compound administration biosamples; D^W, detected in WDS administration biosamples.*

(**Figure 3**), including 18 withanolides, 14 withanolide glucosides, six amides, one indole, one triterpenoid, one steroid, and one sesquiterpenoid. Among them, 17 compounds (**1**, **3**, **5**, **9**, **10**, **13**, **18**, **19**, **20**, **22**, **29**, **30**, **31**, **32**, **36**, **40**, and **41**) were unambiguously identified by a comparison with reference standards. Another 25 potential constituents (**2**, **4**, **6**, **7**, **8**, **11**, **12**, **14**, **15**, **16**, **17**, **21**, **23**, **24**, **25**, **26**, **27**, **28**, **33**, **34**, **35**, **37**, **38**, **39**, and **42**) were tentatively characterized based on their retention times, UV spectra, high-accuracy mass spectra, and MS/MS fragmentation behaviors. Chemical structures of the single compounds characterized in WDS are given in **Figure 2**.

Metabolic Pathways of Single Representative Compounds

The chemical constituents of WDS were classified into seven groups according to their structural type: withanolides (A), withanolide glucosides (B), amides (C), indoles (D), triterpenoids (E), steroids (F), and sesquiterpenoids (G). In our previous study, we selected four representative compounds containing two withanolide glucosides (daturataturin A and daturametelin I), and two amides (cannabisin F and *n*-trans-feruloyltyramine) from WDS and elucidated their metabolic pathways (Xu et al., 2018). In the present study, we used these pathways for metabolite identification of other compounds, which had similar scaffolds in WDS, developing a "compound to extract" strategy. The metabolic pathways of daturametelindole B (**1**), daturametelin M (**3**), hyoscyamilactol (**5**), daturametelindole A (**9**), dinoxin B (**10**), withametelin L (**13**), daturametelindole D (**18**), cinerolide (**20**), daturametelindole C (**22**), daturametelin L (**29**), daturaolone (**32**), *n*-trans-p-coumaroyltyramine (**40**), and stigmasterol (**41**) were first reported in this study, and these 13 single compounds were selected to represent seven major scaffolds in WDS. These compounds were labeled in the HPLC fingerprint of WDS. As shown in **Table 1**, the multistage mass spectrum fragmentation information (ESI-MS^n) was obtained both from UPLC/ESI/qTOF-MS and Q TRAP LC/MS/MS analysis.

Withanolides

Compounds **3**, **5**, and **13** were chosen as representatives of withanolides (**Figure 2**). They were considered as bioactive constituents (Ma et al., 1999; Zhang et al., 2018) and could be detected *per se* in plasma and urine samples. Hydroxylation was the major metabolic reaction for withanolides from *D. metel* (**Table 1**). In addition, compounds **3** and **5** may be metabolized into 21-OH daturametelin M and 21-OH hyoscyamilactol, respectively. This reaction was also observed for daturataturin A (**36**) and daturametelin I (**30**) in our previous study (Xu et al., 2018). However, the hydroxyl position of **13** could not be assigned due to the limited structural information. Hydroxylated products were also detected when **3**, **5**, and **13** were incubated in rat liver microsomes, indicating that the hydroxylation reaction was catalyzed by P450 enzymes (**Supplementary Figure S1**).

Withanolide Glucosides

The metabolism of two withanolide glucosides, **10** and **29**, was investigated. When *O*-glycosides lose the sugar residue to produce corresponding aglycones (withanolides),

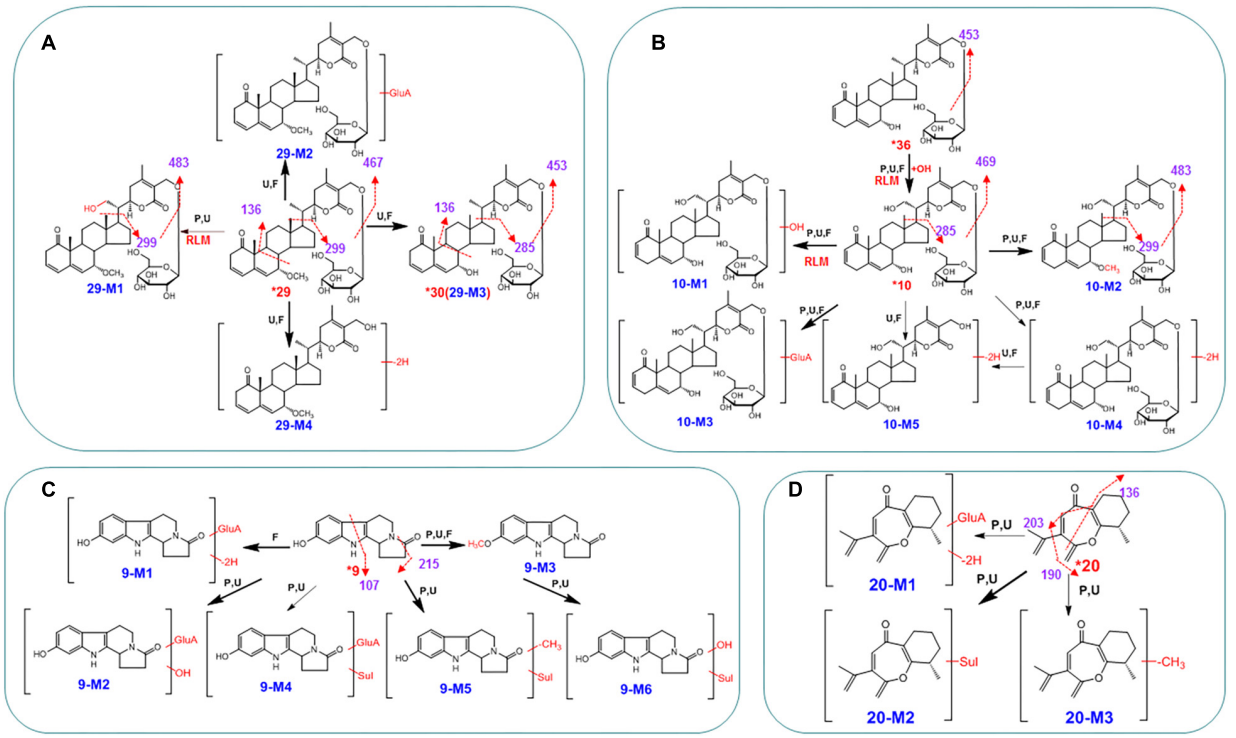

FIGURE 4 | The proposed metabolic pathways for compounds **9 (C)**, **10 (B)**, **20 (D)**, and **29 (A)** in rats after the oral administration of the WDS. Red bold arrows indicate major metabolites; *, compared with reference standards; U, detected in urine samples; P, detected in plasma samples; F, detected in fecal samples; RLM, detected in rat liver microsomes; Sul, sulfate; GluA, glucuronic acid residue.

dehydrogenation occurs. This reaction of interconversion was very common for withanolide glucosides. In addition, hydroxylation, (de)methylation, and glucuronidation of withanolide glucosides were also major reactions as shown in **Figures 4A,B**. These metabolites, derived from the three withanolide glucosides, were detected in plasma, urine, and fecal samples (**Table 1**). For example, **29** produced the hydroxylated metabolite **29-M1** (*m/z* 647→483, 469, 299, 136), the demethylated metabolite **29-M3** (*m/z* 617→453, 285, 136, identified as **30**), the glucuronide-conjugated metabolite **29-M2** (*m/z* 807→631, 453, 285, 136), and hydrolyzed and dehydrogenated metabolite **29-M4** (*m/z* 466→453, 285, 134).

Amides

Amides are abundant in *D. metel* seeds, and considered as characteristic components (Karim et al., 2017). Four major amides (**1**, **18**, **22**, and **40**) were chosen to examine the *in vivo* metabolism of this type of compounds. In brief, the metabolism of amides varied significantly according to the group substitutions on their backbones. For example, **1** and **40** could undertake different phase I reactions, including hydroxylation, dehydrogenation, hydroxylation, and hydration. Phase II conjugation reactions (to form glucuronides and sulfates) were common in amides (**Table 1**), but the peaks of glucuronides disappeared when the sample was treated with β-glucuronidase (**Supplementary Figure S2**). Amides **18** and **22** were mainly involved in demethylation and sulfation. The major metabolic reactions and metabolite distributions of these four amides are listed in **Table 1**. Plasma and urine samples mainly contained phase II metabolites and hydroxylated products, while urine samples comprised most metabolites.

Indoles

Indole alkaloids in *D. metel* seeds are extremely important, and their distribution and metabolism have been reported in several different organisms (Gillam et al., 2000; van der Fits and Memelink, 2000; Rischer et al., 2006; Ziegler and Facchini, 2008). We chose daturametelindole A (**9**) for examining metabolic pathways. The qTOF mass spectra showed $[M+H]^+$ ions at *m/z* 243.1116, consistent with the molecular formula of $C_{14}H_{14}N_2O_2$. In the ion trap MS^n spectra, the $[M+H]^+$ ions could further add a glucuronic acid moiety (176 U), and then be dehydrogenized, hydroxylated, and sulfated to produce the corresponding ions at *m/z* 417 (**9-M1**), 435 (**9-M2**), and 499 (**9-M4**), respectively (**Figure 4C**). The above conjugates were confirmed by enzyme hydrolysis. When indole **9** from the plasma sample was treated with β-glucuronidase, the peaks of **9-M1**, **9-M2**, and **9-M4** disappeared, and the peak corresponding to **9** increased remarkably (**Figure 4C**). Thus, it could be deduced that these metabolites were glucuronides of **9**. The sulfate conjugates **9-M5** and **9-M6** were detected in plasma, urine, and fecal samples. Their MS/MS spectra were dominated by the neutral loss of 80 Da. Metabolite **9-M3** was highly abundant in fecal samples. Its high-resolution mass spectra

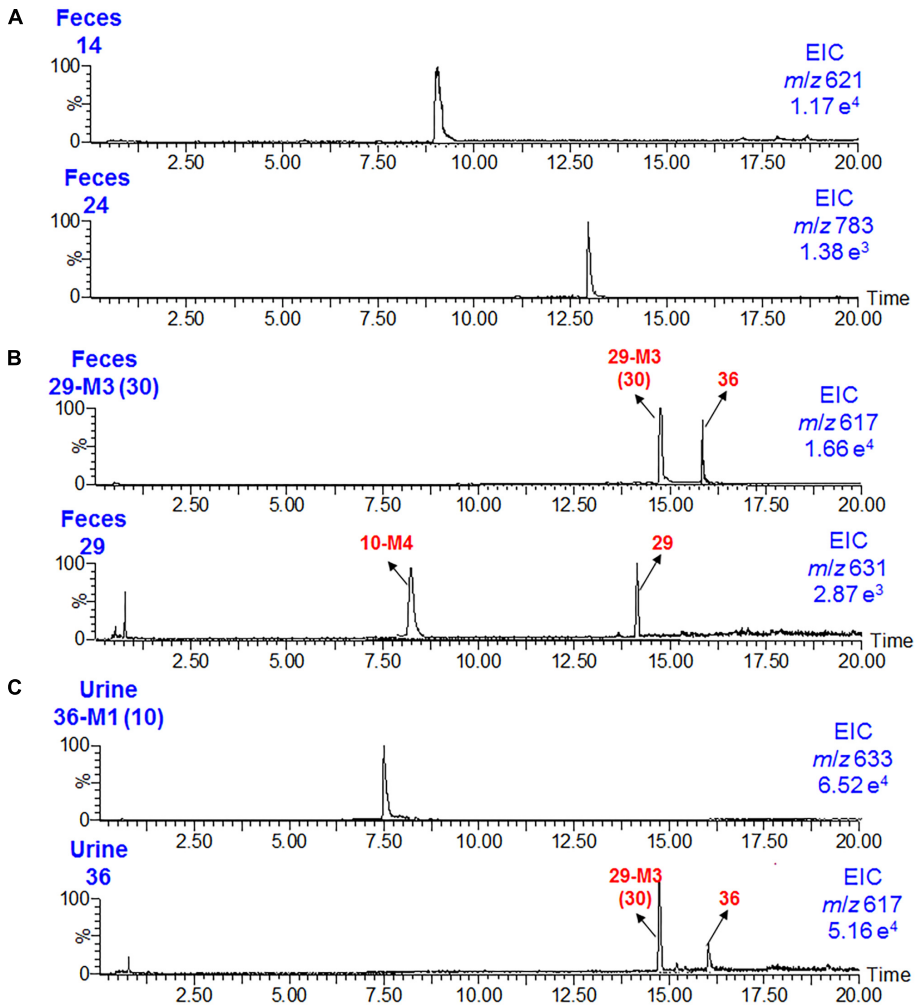

FIGURE 5 | Ion chromatograms of **14** and **24 (A)**, **29-M3** (**30**), and **29 (B)** in rat fecal samples, and of **36-M1** (**10**) and **36 (C)** in rat urine samples after the oral administration of the WDS.

showed an $[M+H]^+$ ion at *m/z* 257.1296, corresponding to the molecular formula $C_{15}H_{16}N_2O_2$. In the tandem mass spectra, **9-M3** produced fragment ions at *m/z* 243 ($[M+H\text{-}CH_3]^+$), *m/z* 215 ($[M+H\text{-}CH_3\cdot\text{-}CO]^+$), and *m/z* 107 ($[M+H\text{-}CH_3\text{-}CO\text{-}C_7H_9N]^+$), indicating that it was methylated metabolite. The metabolic pathways of **9** are illustrated in **Figure 4C**.

Triterpenoids, Steroids, and Sesquiterpenoids

In addition to the major structural types (A) to (D), less abundant groups of compounds were also found in WDS in previous chemical studies (Kuang et al., 2009; Yang et al., 2014; Bhardwaj et al., 2016). They were taken into consideration in this study, and the representative scaffolds included triterpenoids (**32**, daturaolone), steroids (**41**, stigmasterol), and sesquiterpenoids (**20**, cinerolide). Identification of **32**, **41**, and **20** is depicted in **Table 1**.

When **32** was provided to rats, high amounts of prototype were detected in fecal samples. The methoxyl groups at C-23, -14, -29, or -30 may undergo hydroxylation, followed by glucuronide conjugation (**Table 1**; Sanchez-Gonzalez et al., 2015). The phase I and phase II metabolites of **41** were also observed *in vivo* samples. Among phase I metabolites, the hydroxylation products were extensively observed. This type of reaction involved the addition of one or two hydroxyl groups to the parent drug. The phase II biotransformation was mainly sulfation, and the phase II metabolite **41-M3** was formed by a reduction reaction followed by a sulfated reaction. Most steroids were metabolized in the same way as ganoderic acid D (Cheng et al., 2012). After 20 mg/kg oral administration, a large portion of **20** was metabolized. Although this compound was not observed in plasma samples, it occurred in the unchanged form in fecal samples. The UPLC/ESI/qTOF-MS analysis detected large proportions of three metabolites in plasma samples (**Table 1**). The high-resolution mass spectra of **20-M3** revealed a $[M+H]^+$ signal at *m/z* 217.1211, indicating the molecular formula $C_{14}H_{16}O_2$, corresponding to a demethylated derivative of **20**. Similar to cyperon (Duan et al., 2012), **20** presented fragment ions at *m/z* 231 ($[M+H\text{-}O]^+$), 203 ($[M+H\text{-}CO]^+$), and 190

($[M+H-C_3H_5]^+$) (**Figure 4D**). Two phase II metabolites of **20** were detected, namely, glucuronide conjugate (**20-M1**) and sulfate conjugate (**20-M2**) (**Figure 4D**), which disappeared when the sample was treated with β-glucuronidase.

Characterization of WDS Metabolites at a Clinical Dosage

To mimic traditional Chinese medicine clinical use, *D. metel* seeds were cooked in water to obtain the WDS extract. The dosage of WDS provided to rats (0.15 g/kg) was equivalent to the 1.5 g/day for a 60-kg human (Pharmacopoeia Commission, 2015). Under these conditions, 61 metabolites (including intact original compounds) were detected in rat plasma samples, 83 in urine samples, and 76 in fecal samples using qTOF-MS and LC/MS/MS. Withanolides, withanolide glucosides, and alkaloids were the major absorbed chemical components of WDS, and their oral bioavailability was as follows: withanolides >withanolide glucosides >amides and indoles. The contents of compounds **9**, **13**, and **20** are very high in WDS, and they could also be easily detected in WDS-administrated plasma samples. Interestingly, as shown in **Table 1** and **Figure 5**, withanolide monoglucoside (**14**) appeared to have a better oral bioavailability than withanolide diglucoside (**24**). In addition, hydroxylation or (de)methylation was the most common reaction for withanolide glucosides. The absorption of the demethylated metabolite occurred at 7-OH (for instance **29-M3**, **30**) was easier than the prototypes (**29**); besides that, the hydroxylated metabolite at C-21 (**36-M1**, **10**) could be readily absorbed into circulation than compound *per se* (**36**) (**Figures 4**, **5**).

Overall, and according to the metabolic pathways of single representative compounds, the major reactions of the WDS extract included phase II metabolism, hydroxylation, (de)methylation, and dehydrogenation. The phase II metabolites were confirmed by β-glucuronidase hydrolysis. The hydroxylation of **3**, **5**, **10**, **13**, **29**, **40**, and **41** was confirmed by rat liver microsomes incubation experiments, indicating that this hydroxylation was catalyzed by P450 enzymes. Withanolides and withanolide glucosides without a phenolic hydroxyl group at C-21 might readily undergo monohydroxylation. Compounds **9**, **10**, and **36** could add a methyl group, and compounds **20**, **21**, **28**, and **31** could lose a methyl group. Finally, five dehydrogenated metabolites (**1-M5**, **4-M2**, **10-M4**, **12-M5**, and **19-M3**) were characterized by LC/MS analysis (**Table 1**). Among the metabolic reactions described above, the phase II metabolism (glucuronidation or sulfation) was observed most commonly in the metabolism of WDS constituents.

CONCLUSION

We propose the strategy "chemical analysis, metabolism of single representative compounds, and metabolism of the extract at the clinical dosage" to systematically characterize the *in vivo* metabolites of *D. metel* seeds. After the oral administration of *D. metel* seeds water extract to rats at a normal clinical dosage (0.15 g/kg), 113 phytochemicals (including intact original compounds) were identified or tentatively characterized by a highly sensitive LC/MS-MS method. As far as we know, this is the first report on the full metabolic profiling of the *D. metel* seeds water extract *in vivo*. This strategy could be helpful for pharmacokinetic studies of multi-component herbal products.

ETHICS STATEMENT

The animal facilities and protocols were approved by the Animal Care and Use Committee of Harbin Medical University. All procedures were in accordance with the National Institutes of Health Guide for the Care and Use of Laboratory Animals (ILAR, 1996).

AUTHOR CONTRIBUTIONS

QW, BY, and CX participated in research design. CX, YL, HQ, LN, YZ, WL, XX, and YS conducted the experiments. QW, CX, and YL performed the data analysis.

FUNDING

This work was supported by China Postdoctoral Science Fund (Grant No. 2018M630377), Fundamental Research Funds for the Provincial Universities (Grant No. 2017JCZX59), and Doctoral Fund of The 2nd Affiliated Hospital of Harbin Medical University (Grant No. BS2011-19).

SUPPLEMENTARY MATERIAL

The Supplementary Material for this article can be found online at: https://www.frontiersin.org/articles/10.3389/fphar.2019.00571/full#supplementary-material

REFERENCES

Bachheti, R. K., Rai, I., Mishra, V. K., and Joshi, A. (2018). Antioxidant and antimicrobial properties of seed oil of Datura metel. *J. Environ. Biol.* 39, 182–188. doi: 10.22438/jeb/39/2/mrn-341

Bellila, A., Tremblay, C., Pichette, A., Marzouk, B., Mshvildadze, V., Lavoie, S., et al. (2011). Cytotoxic activity of withanolides isolated from Tunisian Datura metel L. *Phytochemistry* 72, 2031–2036. doi: 10.1016/j.phytochem.2011.07.009

Bhardwaj, K., Kumar, S., and Ojha, S. (2016). Antioxidant activity and FT-IR analysis of Datura innoxia and Datura metel leaf and seed methanolic extracts. *Afr. J. Tradit. Complem.* 13, 7–16. doi: 10.21010/ajtcam.v13i5.2

Cheng, C. R., Yang, M., Yu, K., Guan, S. H., Tao, S. J., Millar, A., et al. (2012). Identification of metabolites of ganoderic acid D by ultra-performance liquid chromatography/quadrupole time-of-flight mass spectrometry. *Drug Metab. Dispos.* 40, 2307–2314. doi: 10.1124/dmd.112.047506

Duan, S. N., Qi, W., Zhang, S. W., Huang, K. K., and Yuan, D. (2012). Ultra high performance liquid chromatography coupled with electrospray ionization/quadrupole time-of-flight mass spectrometry for the rapid analysis of constituents in the traditional Chinese

medicine formula Wu Ji Bai Feng Pill. *J. Sep. Sci.* 40, 3977–3986. doi: 10.1002/jssc.201700438

Gillam, E. M. J., Notley, L. M., Cai, H. L., De Voss, J. J., and Guengerich, F. P. (2000). Oxidation of indole by cytochrome P450 enzymes. *Biochemistry* 39, 13817–13824. doi: 10.1021/bi001229u

Gu, M., Yu, Y., Gumaherath, G., Gunatilaka, A., Li, D., and Sun, D. (2014). Structure-activity relationship (SAR) of withanolides to inhibit Hsp90 for its activity in pancreatic cancer cells. *Invest. New Drugs* 32, 68–74. doi: 10.1007/s10637-013-9987-y

ILAR (1996). *Guide for the Care and Use of Laboratory Animals [EB/OL]*. Washington, DC: National Academy Press. Available at: http://oacu.od.nih.gov/regs/guide/guide.pdf

Kamaraj, C., Rahuman, A. A., Elango, G., Bagavan, A., and Zahir, A. A. (2011). Anthelmintic activity of botanical extracts against sheep gastrointestinal nematodes, *Haemonchus contortus*. *Parasitol. Res.* 109, 37–45. doi: 10.1007/s00436-010-2218-y

Karim, M., Jabeen, K., Iqbal, S., and Javaid, A. (2017). Bioefficacy of a common weed Datura metel against *Colletotrichum gloeosporioides*. *Planta Daninh* 35:e017164676.

Kuang, H. X., Yang, B. Y., Tang, L., Xia, Y. G., and Dou, D. Q. (2009). Baimantuoluosides A-C, three new withanolide glucosides from the flower of Datura metel L. *Helv. Chim. Acta* 92, 1315–1323. doi: 10.1002/hlca.200800404

Kuang, H. X., Yang, B. Y., Xia, Y. G., and Feng, W. S. (2008). Chemical constituents from the flower of Datura metel L. *Arch. Pharm. Res.* 31, 1094–1097. doi: 10.1007/s12272-001-1274-6

Ma, C. Y., Williams, I. D., and Che, C. T. (1999). Withanolides from *Hyoscyamus niger* seeds. *J. Nat. Prod.* 62, 1445–1447.

Mai, N. T., Cuc, N. T., Anh, H. L. T., Nhiem, N. X., Tai, B. H., Yen, P. H., et al. (2017). Two new guaiane sesquiterpenes from Datura metel L. with anti-inflammatory activity. *Phytochem. Lett.* 19, 231–236. doi: 10.1016/j.phytol.2017.01.011

Murthy, B. K., Nammi, S., Kota, M. K., Rao, R. V. K., Rao, N. K., and Annapurna, A. (2004). Evaluation of hypoglycemic and antihyperglycemic effects of Datura metel (Linn.) seeds in normal and alloxan-induced diabetic rats. *J. Ethnopharmacol.* 91, 95–98. doi: 10.1016/j.jep.2003.12.010

Pharmacopoeia Commission (2015). *Pharmacopoeia of the People's Republic of China*, Vol. I. Beijing: Chinese Medical Science and Technology Press, 267.

Rischer, H., Oresic, M., Seppanen-Laakso, T., Katajamaa, M., Lammertyn, F., Ardiles-Diaz, W., et al. (2006). Gene-to-metabolite networks for terpenoid indole alkaloid biosynthesis in Catharanthus roseus cells. *Proc. Natl. Acad. Sci. U.S.A.* 103, 5614–5619. doi: 10.1073/pnas.0601027103

Roy, S., Samant, L., Ganjhu, R., Mukherjee, S., and Chowdhary, A. (2018). Assessment of in vivo antiviral potential of Datura metel Linn. extracts against rabies virus. *Pharmacognosy Res.* 10, 109–112. doi: 10.4103/pr.pr_121_17

Sanchez-Gonzalez, M., Lozano-Mena, G., Parra, A., Juan, M. E., and Planas, J. M. (2015). Identification in rat plasma and urine by linear trap quadrupole-orbitrap mass spectrometry of the metabolites of maslinic acid, a triterpene from olives. *J. Agr. Food Chem.* 63, 1126–1132. doi: 10.1021/jf505379g

van der Fits, L., and Memelink, J. (2000). ORCA3, a jasmonate-responsive transcriptional regulator of plant primary and secondary metabolism. *Science* 289, 295–297. doi: 10.1126/science.289.5477.295

Wannang, N. N., and Ndukwe, H. C. (2009). Evaluation of the analgesic properties of the Datura metel seeds aqueous extract. *J. Med. Plants Res.* 4, 192–195.

Xu, S. L., Liu, Y., Xiang, L., Zhou, F., Li, H. Y., Su, Y. J., et al. (2018). Metabolites identification of bioactive compounds daturataturin A, daturametelin I, n-trans-feruloyltyramine, and cannabisin F from the seeds of Datura metel in rats. *Front. Pharmacol.* 9:731. doi: 10.3389/fphar.2018.00731

Yang, B. Y., Xia, Y. G., Liu, Y., Li, L., Jiang, H., Yang, L., et al. (2014). New antiproliferative and immunosuppressive withanolides from the seeds of Datura metel. *Phytochem. Lett.* 8, 92–96. doi: 10.1016/j.phytol.2014.02.008

Yang, B. Y., Xia, Y. G., Wang, Q. H., Dou, D. Q., and Kuang, H. X. (2010a). Baimantuoluosides D-G, four new withanolide glucosides from the Flower of Datura metel L. *Arch. Pharm. Res.* 33, 1143–1148. doi: 10.1007/s12272-010-0802-4

Yang, B. Y., Xia, Y. G., Wang, Q. H., Dou, D. Q., and Kuang, H. X. (2010b). Two new amide alkaloids from the flower of Datura metel L. *Fitoterapia* 81, 1003–1005. doi: 10.1016/j.fitote.2010.06.017

Zhang, H., Bazzill, J., Gallagher, R. J., Subramanian, C., Grogan, P. T., Day, V. W., et al. (2018). Antiproliferative withanolides from Datura wrightii. *Planta Med.* 79, 861–862.

Ziegler, J., and Facchini, P. J. (2008). Alkaloid biosynthesis: metabolism and trafficking. *Annu. Rev. Plant Biol.* 59, 735–769. doi: 10.1146/annurev.arplant.59.032607.092730

Conflict of Interest Statement: The authors declare that the research was conducted in the absence of any commercial or financial relationships that could be construed as a potential conflict of interest.